Geophys. J. Int. (1993) **114,** 561–568

The effect of sea tides on gravity tidal observations on the Antarctic Ekström ice shelf

Bülent Tezkan[1] and Ugur Yaramanci[2]

[1] *Alfred-Wegener-Institut für Polar und Meeresforschung, Columbusstrasse, 2850 Bremerhaven, Germany*
[2] *GSF-Forschungszentrum für Umwelt und Gesundheit, Theodor-Heuss-Strasse 4, 3300 Braunschweig, Germany*

Accepted 1993 January 29. Received 1993 January 21; in original form 1992 March 2

SUMMARY

Simultaneous time series of gravity variations on an ice shelf and sea-level fluctuations in the Antarctic have been analysed. The gravity data was recorded in the observatory of the Georg von Neumayer (GvN) station on the Ekström ice shelf in the Antarctic by an Askania GS-15 earth-tide gravity meter. An Aanderaa pressure recorder was used on a mooring 10 km north of the ice-shelf edge in a water depth of 468 m to measure the sea-level fluctuations. Both time series are approximately one year in length. Amplitudes and phases for the tidal waves and residual spectra, with minimum leakage effects, were obtained using the least-squares method of the HYCON program. The gravity variations on the ice shelf are primarily caused by the local sea tides. The amplitude of the main tidal wave M_2 is 80.3 μgal (1 μgal = 10^{-8} ms^{-2}). After removing the effect of the body and load tide the residual signal of 89.7 μgal amplitude corresponds to a tidal height of 33 cm while the tidal acceleration is only 8.3 μgal. The vertical movement of the ice shelf is modelled by a simple elastic model. The ice shelf is taken as a uniform elastic beam floating on the sea and clamped on one side. This model constrains the location of the hinge zone of the Ekström ice shelf to be about 55 km south of the GvN station and verifies the observed vertical displacements at this station.

Key words: Antarctica, Ekström ice shelf, elastic beam model, gravity tides, sea tides, tidal analysis.

1 INTRODUCTION

Simultaneous sea-level and gravity observations on an ice shelf have a number of objectives. In this study time series of both will be used to determine a transfer function that characterizes the vertical movement of the ice shelf. The Ekström ice shelf in the Antarctic is a large body of ice which is floating on water and partly resting on earth.

On the earth the difference between the Newtonian attraction of the tide-generating body acting at an observation point and at the earth's centre causes a tidal variation in the earth's gravity field. In addition to the earth's response to the astronomical forces (the body tide) there are further signals arising from the deformation caused by loads and from the mass attraction of oceanic tides (e.g. Wilhelm & Zürn 1984). These signals are not easily distinguished from the body tides because their frequencies are the same, all resulting from the same astronomical input.

Figure 1 shows the amplitude variation of the main tidal-gravity waves as a function of latitude (Melchior 1982). Small amplitudes of semi-diurnal waves are expected at the location of the GvN station, whereas amplitudes of diurnal waves should be greater.

However, gravity-tide measurements on ice shelves may primarily be sensitive to the vertical movement of the ice as the shelf is deformed by the buoyant load exerted by the local sea tide. Shelf ice movements have been shown to occur in the following Antarctic locations: Quar ice shelf (Robin 1958), Filchner–Ronne ice shelf (Pratt 1960; Eckstaller & Miller 1984), Ross ice shelf (Thiel *et al.* 1960; Robinson *et al.* 1977; Williams & Robinson 1979), Lazarew ice shelf (Dubrovin & Simonov 1965), George VI ice shelf (Bishop & Walton 1977), and Ekström ice shelf (Kobarg 1988).

Due to logistic difficulties in the polar regions the former studies were restricted to observations of gravity variations on the ice shelves. In order to get information about the local ocean tides and to study the vertical movement of the Ekström ice shelf due to the ocean tides, a recording pressure gauge was installed on a mooring 10 km north of the edge of the Ekström ice shelf.

The aim of the present paper is to use the gravimetric

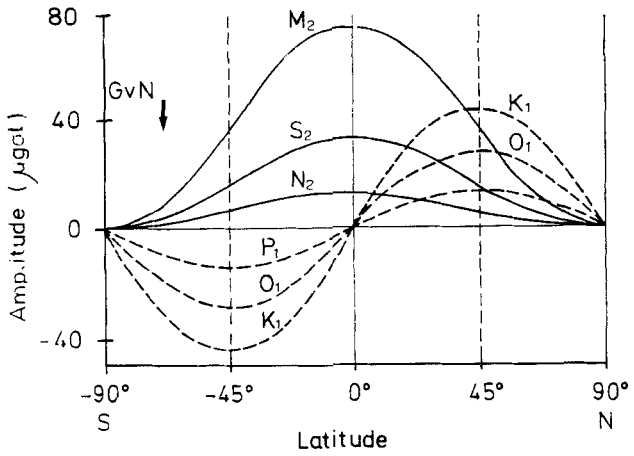

Figure 1. Latitude dependence of the amplitudes of K_1, O_1, P_1 (diurnal waves) and of M_2, S_2, N_2 (semi-diurnal waves) for the gravity-tide component of the tidal force (Melchior 1982). The latitude of the GvN station is 70°36'S.

measurements to deduce the vertical-tide-driven motion of the Ekström ice shelf at the GvN station, compare this motion with the displacement of the shelf edge as inferred from a pressure-gauge record, then using the difference between both determine the location of the hinge zone of the Ekström ice shelf using a simple elastic beam model and verify the observed vertical displacements at the GvN station.

Tidal gravity on the Ekström ice shelf was also a major issue in Kobarg (1988) who applied a bending-slab model to tilt measurements rather than vertical motion invoking viscoplastic rheology.

Major new ingredients in the present paper are the use of sea-bottom pressure measurements for the modelling and the application of the ice-slab model to the vertical motion rather than tilt.

2 LOCATION OF THE STATIONS AND INSTRUMENTATION

The Ekström ice shelf is one of the smaller ice shelves in the Antarctic. It hosts the GvN station which is located 7 km west of the Atka ice port at 70°36'S and 8°22'W (Fig. 2). In the geophysical observatory of the station, an Askania GS-15 earth-tide gravity meter measures since 1982 the variation of gravity caused by the vertical component of the tidal force. The movements of the ice shelf are not restricted to the tidal frequencies. Significant signal energy is found as a background in a wide spectral range. Signals at higher frequencies are caused by earth- or icequakes. They are suppressed by an electronic lowpass filter with a cut-off period of 300 s. The quasi-periodic signals are produced by the swell (Kobarg 1988) and have periods of 10–20 s and amplitudes of 5–10 mgal. A feedback was added to the gravimeter system in order to maintain the sensor position within a range of linear response.

Radar measurements on the Ekström ice shelf showed that the ice beneath the station is 200 m thick and the water beneath the ice shelf has a depth of about 120 m (Thyssen & Grosfeld 1988). The ice thickness increases rapidly to the

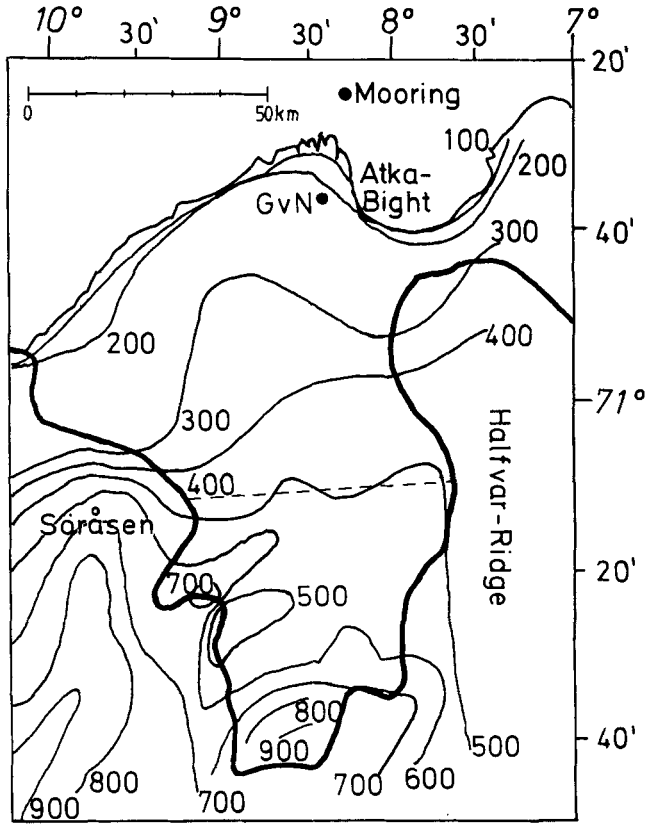

Figure 2. Map of ice thickness of the Ekström ice shelf after Thyssen & Grosfeld (1988) showing the location of the GvN station and the position of the mooring. The dashed line shows the hypothetical hinge zone.

south (Fig. 2). The lateral edges of the ice shelf, the Söråsen and the Halfvar Ridge rest on the continent. The dashed line in Fig. 2 shows the hinge zone as determined in this study.

In order to obtain information about the local ocean tides a mooring was installed at 70°25.75'S and 8°17.5'W at a water depth of 468 m. (Krause 1988). Hourly data samples were automatically stored on magnetic tapes.

3 PRESENTATION AND ANALYSIS OF OBSERVED TIME SERIES

The Aanderaa pressure recorder obtained 7776 hourly samples between 1987 February 27 and 1988 January 16. A data record of 8736 hourly samples starting also on 1987 February 27 was chosen from the continuous registration of the Askania GS-15 earth-tide gravity meter.

The data quality for the sea level time series is excellent (Fig. 3). They are free of trend and gaps; no preprocessing is required. The gravity record, on the other hand (Fig. 4), had many interruptions and spikes. The latter were deleted and the signal was detrended in order to avoid degradation of the signal-to-noise ratio and bias, respectively. Short gaps of less than two hours were filled by linear interpolation.

There are many ways and methods to determine the amplitudes and phases of the tidal waves (e.g. Melchior 1982). Generally least-square methods are advantagous because they adjust a signal model utilizing well-known tidal-frequency information.

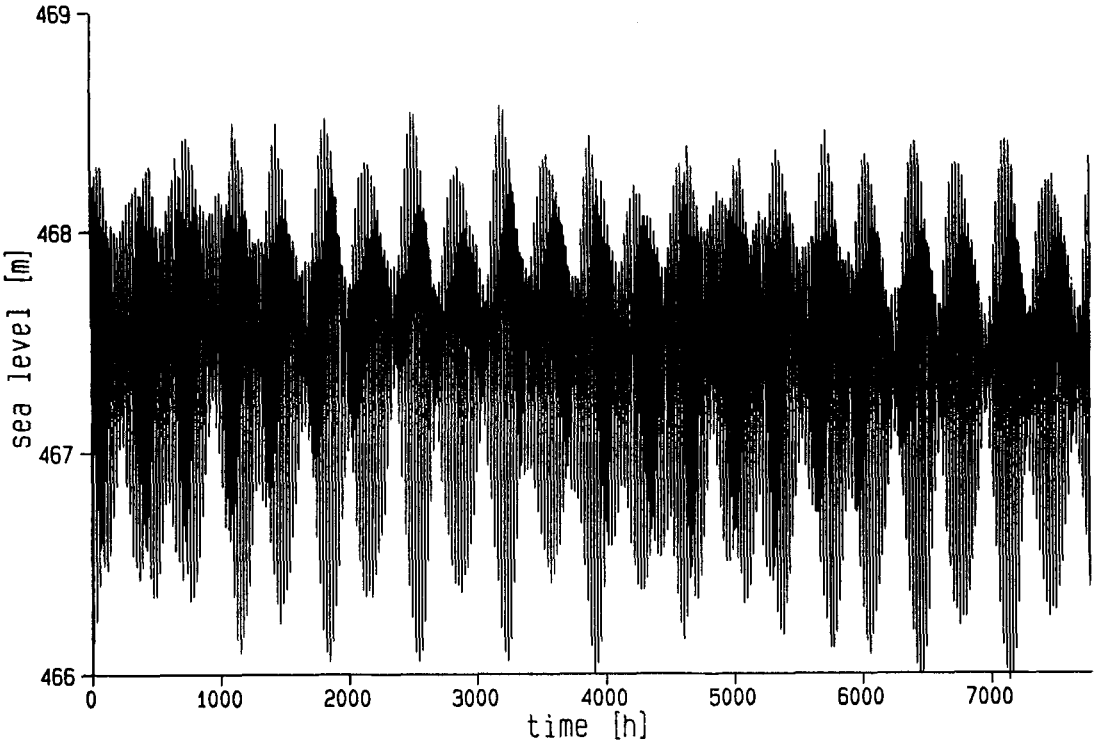

Figure 3. Time series of hourly values of sea-level, measured with Aanderaa pressure recorder in 468 m water depth, in Atka Bight.

We decided to use the HYCON program of Schüller (1976, 1978). Results of its application to the observed gravity and sea-level time series are given in Tables 1 and 2. The classical least-squares method tends to underestimate the true parameter error unless the underlying conditions are fulfilled: observation error is uncorrelated; unmodelled signals and noise components do not correlate with modelled signals (Zürn, Beaumont & Slichter 1976). While the second condition is weaker, it is still possible to infer realistic confidence limits for the case of long-duration sinusoids in coloured noise using spectral analysis of the residual (Schüller 1976). As an option, HYCON code reduces the correlation of signals at different frequencies and the pick up of noise by employing a tapered data

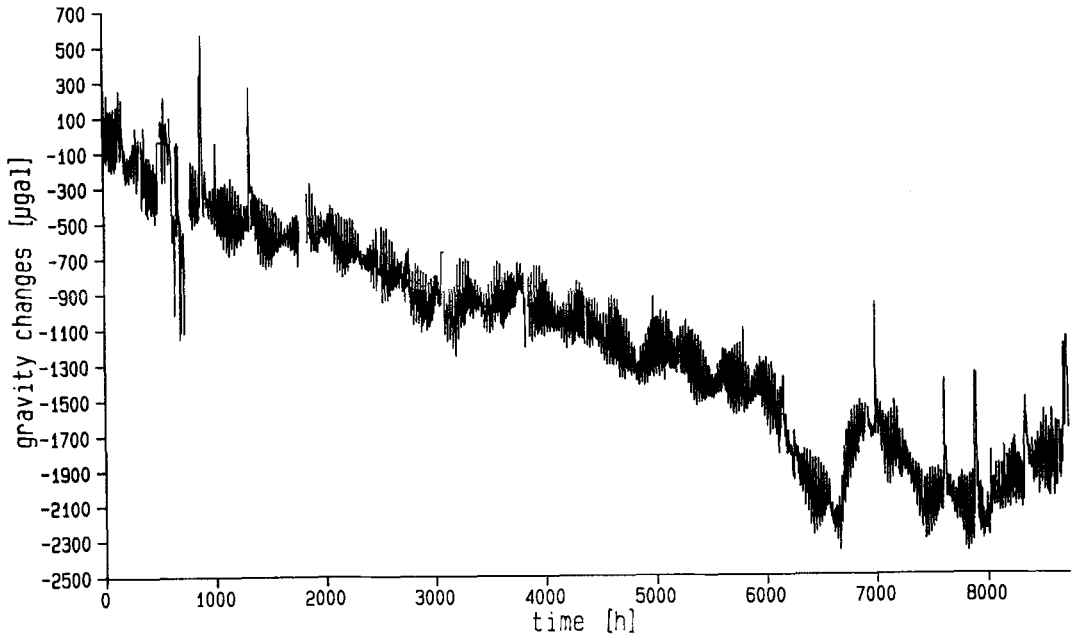

Figure 4. Original time series of hourly values of gravity variations measured on the Ekström ice shelf in the observatory of the GvN station. Before the frequency-domain analysis is carried out, spikes and trend are removed.

Table 1. Observed and theoretical amplitudes (A) and phases (P) of gravity tides at the GvN station for 16 main constituents. The time interval is from 1987 February 27 to 1988 February 25. P_{obs} is related to the beginning of the record.

Tide	Freq.	A_{obs}	A_{err}	A_{theo}	P_{obs}	P_{err}	P_{obs} -P_{theo}
	°/h	μgal	μgal	μgal	deg.	deg.	deg.
SIQ_1	12.3828	1.38	1.82	0.14	171.9	75.5	-133.0
$2Q_1$	12.8543	2.29	1.89	0.49	116.2	47.2	-118.0
σ_1	12.9271	2.86	2.08	0.59	-160.5	41.8	-146.0
Q_1	13.3987	10.94	2.01	3.73	143.4	10.5	-131.1
ρ_1	13.4715	3.62	2.13	0.71	- 87.1	33.7	-113.2
O_1	13.9430	44.96	2.11	19.49	170.1	2.7	-145.4
P_1	14.9589	8.61	2.53	9.07	139.9	16.8	-145.4
K_1	15.0411	33.44	2.25	27.41	-89.3	3.8	-147.2
N_2	28.4397	11.62	1.30	1.59	6.2	6.4	-146.6
M_2	28.9841	80.30	1.46	8.30	31.5	1.0	-161.8
L_2	29.5285	5.80	2.91	0.23	-80.1	28.8	-134.0
T_2	29.9589	3.37	1.39	0.23	-62.9	23.7	-172.6
S_2	30.0000	58.54	1.39	3.87	-24.0	1.4	172.8
K_2	30.0821	16.19	1.07	1.05	-66.0	3.8	178.2
η_2	30.6265	0.81	0.71	0.06	-55.3	50.2	148.3
M_3	43.4762	1.09	1.06	0.05	-59.1	55.6	-79.1

window, e.g. Hanning, however, inevitably sacrificing spectral resolution by a factor of—typically—2. The error levels given in Tables 1 and 2 are based on the variance of the residuals inside the fundamental-tide-frequency bands. They represent the formal error estimates (Schüller 1976; Yaramanci 1978) given the adopted signal model and the conditions mentioned above. In our analysis 504 waves and 24 non-linear waves were used (Cartwright & Tayler 1971; Cartwright & Edden 1973). The waves were set into 51 groups according to the spectral resolution attainable with a record of one year.

Kobarg (1988) has analysed data from the Askania gravimeter at GvN containing 7896 hourly records from 1984 March 17 to 1985 February 10 using a simpler least-square analysis technique with only 18 major tidal constituents. Using a certified widely used procedure, the HYCON program, this work arrives at significantly different amplitudes and phases than Kobarg (1988). These differences are caused by the fact that the HYCON analysis takes into full account the amplitude modulation of the major tidal waves by smaller constituents, while Kobarg's analysis does not (e.g. Rydelek, Knopoff & Zürn 1982; Zürn 1991, personal communications). However, we do not think that our findings of—in some cases—50 per cent lower amplitudes are solely related to the use of a precise potential with 504 waves in 51 wave groups. There might also have been major mishaps in the data preprocessing of the earlier study. We find a stable ratio of 0.8 ± 0.07 between inferred displacement at GvN and sea-tide amplitude at shelf edge for all major wave groups. This indicates a reasonable range

Table 2. Observed amplitudes (A) and phases (B) of sea tides at the mooring in Atka Bight for 16 main constituents. The time interval is from 1987 February 27 to 1988 January 17. P_{obs} is related to the beginning of the record.

Tide	Freq.	A_{obs}	A_{err}	P_{obs}	P_{err}
	°/h	cm	cm	deg.	deg.
SIQ_1	12.3828	0.25	0.09	77.4	107.8
$2Q_1$	12.8543	0.94	0.09	52.0	5.5
σ_1	12.9771	1.37	0.10	153.3	4.3
Q_1	13.3987	6.74	0.10	80.1	0.8
ρ_1	13.4715	1.30	0.10	-169.2	4.6
O_1	13.9430	29.04	0.10	116.2	0.2
P_1	14.9589	8.92	0.13	91.1	0.8
K_1	15.0411	27.03	0.11	-136.2	0.3
N_2	28.4397	6.27	0.16	98.4	1.4
M_2	28.9841	41.14	0.19	130.0	0.3
L_2	29.5285	1.77	0.39	16.4	12.5
T_2	29.9589	1.96	0.17	47.2	5.1
S_2	30.0000	29.92	0.17	87.9	0.3
K_2	30.0821	8.89	0.13	40.5	0.9
η_2	30.6265	0.54	0.09	54.2	9.1
M_3	43.4762	0.42	0.11	132.0	14.5

for our results. Also, the ratio suggests sufficient sensitivity for a study of internal deformation of the shelf ice.

A comprehensive account of the signal spectra is based on Fourier spectra. Figs 5 and 6 show the Fourier spectra of gravity and sea-tide data, respectively. On both spectra, the diurnal and semi-diurnal tides are significant and their amplitudes are large compared to the noise level. The amplitudes of the body tides are marked in Fig. 5, evidencing the large effects on the instrument that the movement of the shelf induces. Particularly in the case of the M_2 tide, the observed amplitude exceeds that of the body tide by a factor of 15. A factor at maximum 1.3 could be expected at a site that is firmly attached to the solid-earth surface.

In order to account for the movement of the gravity meter due to the ice-surface displacement we used

$$\Delta g = \Delta h \frac{\partial g}{\partial z} + 2\pi\rho G\, \Delta h \qquad (1)$$

where the first term expresses the vertical movement of the station in the gravity field and the second term the Bouguer plate correction for the water displacing the ice. Using the gravitational constant $G = 6.67 \times 10^{-11}\,\mathrm{N\,m^2\,kg^{-2}}$, free-air correction $\partial g/\partial z = 0.3086\,\mathrm{mgal\,m^{-1}}$ and a water density of $\rho = 1028\,\mathrm{kg\,m^{-3}}$ in eq. (1), the amplitudes of the ocean-tidal

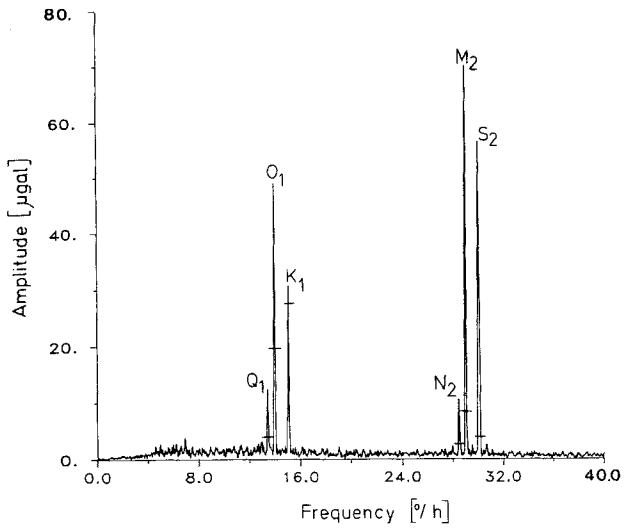

Figure 5. Line spectra of the gravity data observed from 1987 February 27 to 1988 February 15 (see Fig. 4). Note that large amplitudes of diurnal and semi-diurnal tidal waves are observed at the GvN station on the Ekström ice shelf. For comparison the theoretical tidal amplitudes are also indicated as horizontal bars in the spectra.

constituents Δh can then be calculated from the observed gravity tides Δg.

First, the amplitudes of the theoretical gravity tide for the location of the station are multiplied by the gravimetric factor of 1.154 (Wahr 1981), yielding the body tide. The load tides at the GvN station are given for the eight major tidal waves in Table 3 (Agnew & Zürn 1991, personal communication). Both the load tides and the body tides are then subtracted from the observed gravity tides. This procedure is shown as an example for the four major waves in Fig. 7. The amplitudes and phases of the vertical displacements resulting from (1) and tabulated for the main constituents in Table 4, are the target of modelling in Section 4.

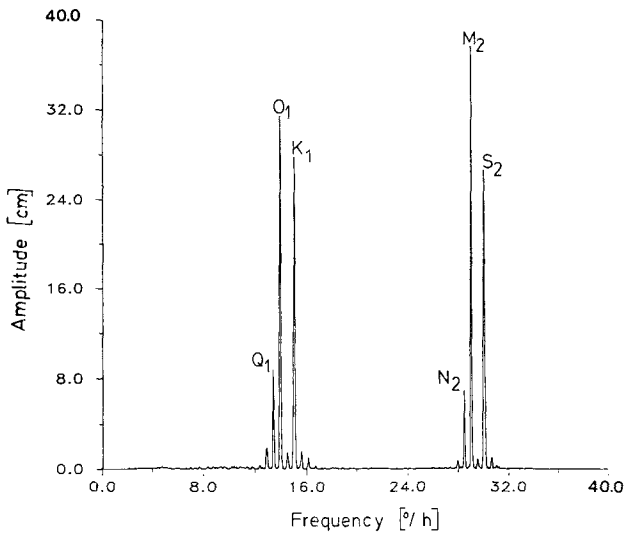

Figure 6. Line spectra of the sea-level data observed from 1987 February 27 to 1988 January 17 (see Fig. 3).

Table 3. Amplitude (A) and phases (P) of the load tides at the GvN station for the eight major tidal waves. The phases are relative to the local theoretical tides with negative lags (Agnew & Zürn, personal communication).

Tide	A	P
	μgal	deg.
Q_1	0.49	-160.7
O_1	2.54	-167.2
P_1	0.70	-175.4
K_1	1.90	-178.0
N_2	0.38	- 18.0
M_2	2.11	- 28.4
S_2	1.84	- 55.0
K_2	0.51	- 65.4

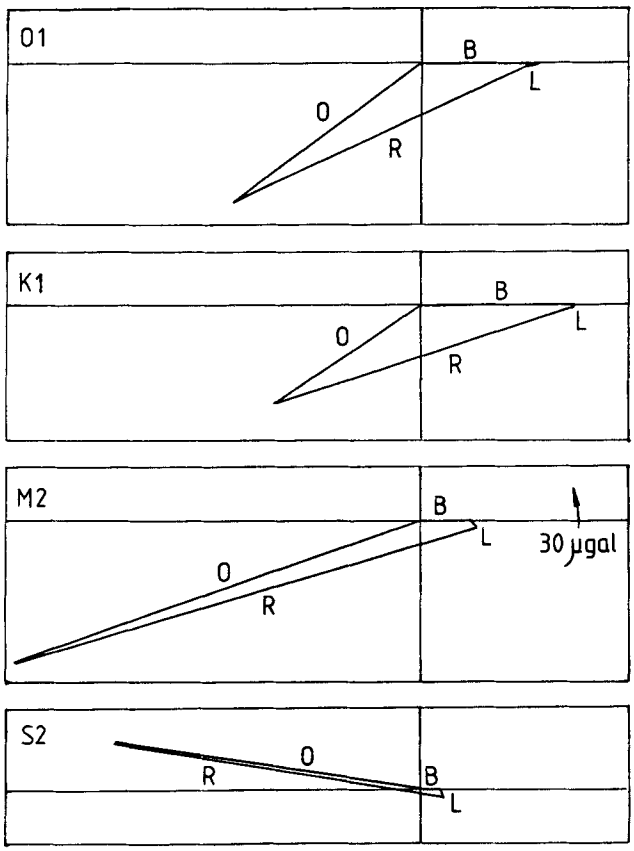

Figure 7. Phasor plots for the large waves O_1, K_1, M_2, S_2. The amplitudes in μgal are plotted radially and the phase lags with respect to the body-tide phase are shown anti-clockwise from 0°. O, B, L are observed, body and load tides. R is the residual tide to be explained by a model $[R = O - (B + L)]$.

Table 4. Observed amplitudes (A) and phases (P) of gravity tides at the GvN station after subtracting body tides and local tides. Amplitudes of sea tides (Z) at the GvN station derived from gravity tides.

	A	P	Z	Z_{err}
	μgal	deg.	cm	cm
Q_1	13.21	-142.3	4.97	0.76
O_1	59.51	-155.2	22.41	0.79
P_1	16.19	-162.6	6.09	0.87
K_1	56.57	-161.4	21.3	0.85
N_2	13.23	-151.7	4.98	0.49
M_2	89.72	-164.4	32.78	0.55
S_2	63.62	172.0	23.9	0.52
K_2	17.47	176.8	6.57	0.40

In order to show the quality of the analysis by the HYCON method, the spectra of the residuals are shown in Figs 8 and 9. In the gravity residual, no significant signal energy is present at the astronomical tide frequencies as evident from Fig. 8(a), the residuals being nearly random. The level of the residual signal in the tidal bands is 1 μgal or less. In the sea-level residual spectra in Fig. 8(b) some energy can be seen at the near-tidal frequencies. This remaining energy can be interpreted as a barometric effect or, alternatively, be induced due to non-linear interaction of the major tidal waves.

Non-linear waves such as SK_3 can indeed be discerned in the spectrum of the gravity residual (Fig. 9a). They have been also reported earlier in Kobarg & Lippmann (1986), who attributed the effect to non-linear response of the local ocean tide rather than non-linear response of the ice slab. The presence of these tides in the ocean-pressure data, as seen in Fig. 9(b), supports this view. However, none of the non-linear waves presents a critical case for our ice-slab model since their amplitudes cannot be determined with the accuracy required. It also remains to be determined whether the ice-slab response itself is linear, or whether the different amplitude ratios of e.g. M_4:MS_4 in gravity and sea level, respectively, can be interpreted as being indicative of ice non-linearity.

4 INTERPRETATION OF THE VERTICAL DISPLACEMENTS AT THE GvN BY A SIMPLE MODEL

The vertical movement of the Ekström ice shelf can be explained as a consequence of in and outflow of tidal water. The ice shelf is taken as an elastic beam, one end of which is fixed (hinge zone), while the whole beam is loaded (Fig. 10).

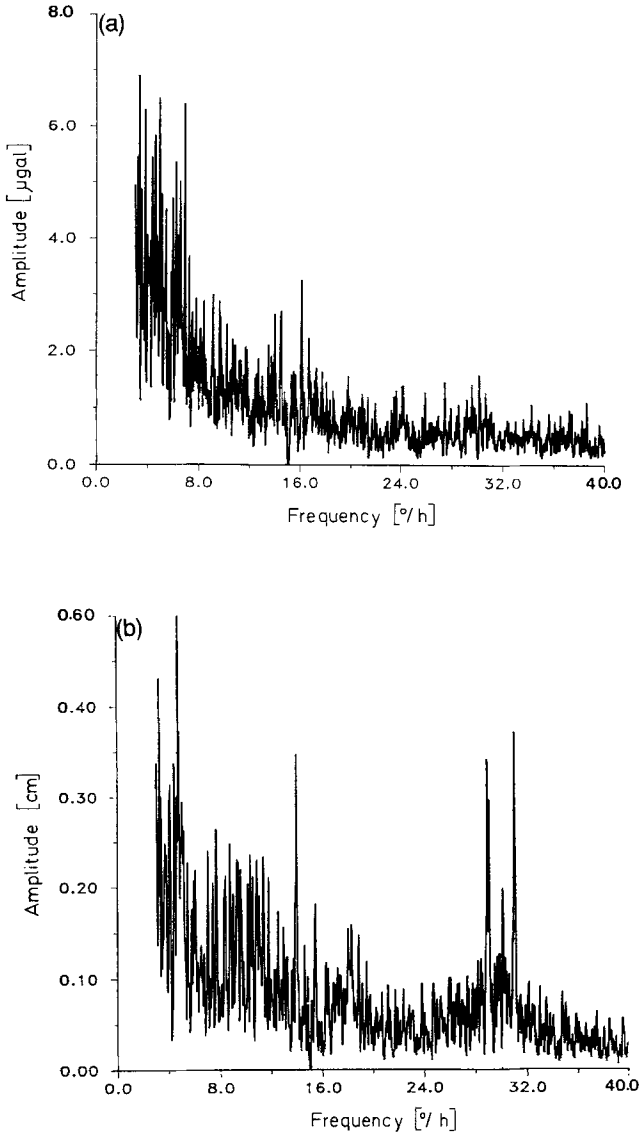

Figure 8. Residual spectra calculated by the HYCON method in the frequency range 0–40°/hr for (a) gravity and (b) sea-level changes. The residuals can be assumed to be random as there are no or very small energies in tidal frequencies.

The load is assumed to be uniformly distributed. The theory of this problem is discussed by e.g. Mende & Simon (1969) and the bending line is given by the equation:

$$Z = Z_0\left[1 - 4\frac{(L-x)}{3L} + \frac{(L-x)^4}{3L^4}\right], \qquad (2)$$

where x is the distance from the hinge zone to the gravity station and L the distance from the hinge zone to the edge of the ice shelf. The maximum observed beam displacement at the edge of the ice shelf, Z_0, may be derived from the observed ocean tides as the sensor was installed sufficiently close to the edge of the ice shelf (Table 2).

The predicted vertical movement is given by Z. The GvN station is situated at $x = L - 10$ km. Its movement due to the tides M_2, O_1, K_1 and K_2 is shown in Fig. 10 using the corresponding Z_0 from Table 2. We let L vary between 10 and 100 km. Also shown in the figure are the observed

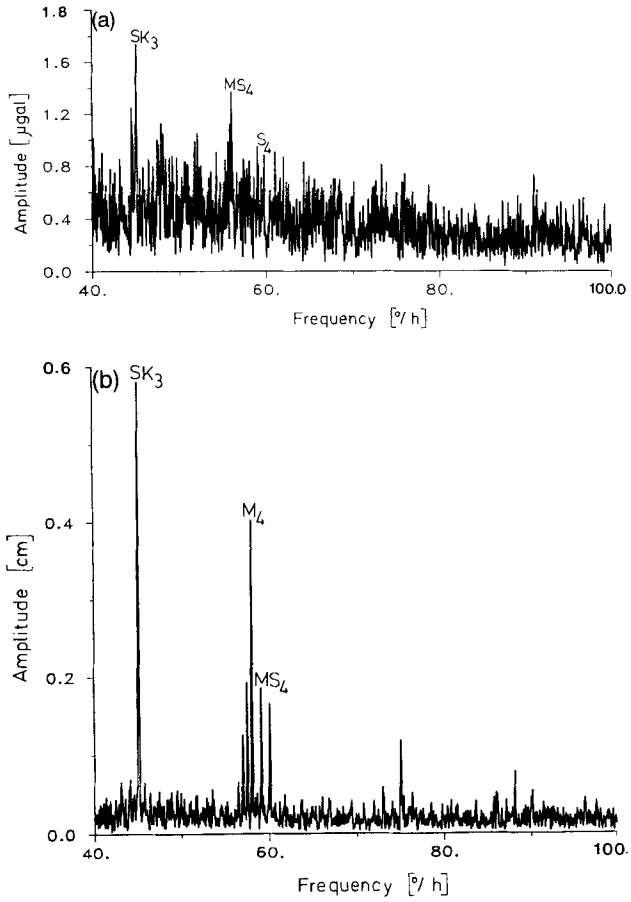

Figure 9. Residual spectra calculated by the HYCON method in the frequency range 40–100°/hr for (a) gravity and (b) sea-level changes. Significant non-linear waves in sea-level signal cause the non-linear waves in the gravity data.

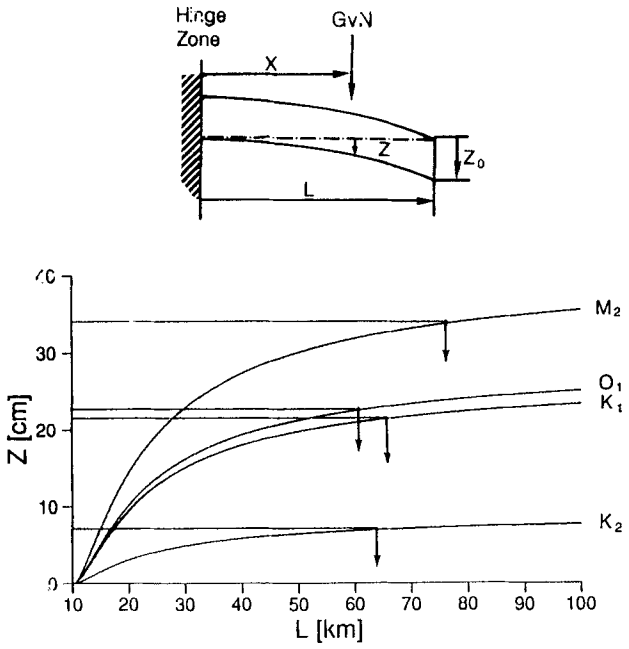

Figure 10. The dependence of the vertical movement Z at the GvN station, which is located 10 km away from the ice-shelf edge, on the distance of the hinge-zone L for the M_2, O_1, K_1 and K_2 waves.

amplitudes at GvN using Table 4. The best fit is obtained with $L \approx 65$ km. This distance coincides with the Halfvar and Söråsen Ridge, which is shown as a dashed line in Fig. 2. The ice thickness is rapidly increasing to the south of this zone; no vertical movement of the ice shelf due to the local ocean tides would be expected there.

In this simple model the ice properties of the Ekström ice shelf have not been taken into account. The model keeps only a simplistic view allowing closed solutions as a first approximation. The distance x from (2) could be still subject to a scaling factor and it is employed to derive a slab of rectangular cross section, however, the wedge shape of the Ekström ice shelf appears complicating. The exact position of clamping would be too difficult to find, lacking data. But the observed stable average ratio of 0.8 between inferred displacement at GvN and sea-tide amplitude at shelf edge for all major wave groups, being nearer to one than to zero, might suggest that it can not be far away and that the deformation takes places predominantly in the thin section of the slab. The observed vertical displacements at the GvN station could also be verified by a viscoplastic model using the theory of tidal bending as discussed by Holdsworth (1977) and by Kobarg (1988), allowing us to estimate values of some ice properties. Tidal bending theory was successfully applied to other Antarctic ice shelves and to glacier tongues (Holdsworth 1969, 1977; Hughes 1975, 1977; Lingle, Hughes & Kollmeier 1981). Especially Kobarg (1988) successfully verified tiltmeter observations on the Ekström ice shelf northwest of the GvN using a viscoplastic model for the ice shelf. The application of such a viscoplastic model to the observations in this study shows some troubles, because no exact viscoplastic solution for the vertical displacement is possible and because approximate solutions as suggested by Holdsworth (1977) have ambiguities concerning some ice properties which are involved in the solution. Due to the mentioned ambiguities of the viscoplastic model the modelling part is limited to a simple elastic model as a first approximation which does not consider the ice properties of the Ekström ice shelf in the solution, but it could verify all the observed vertical displacements at the GvN.

5 CONCLUSION

Gravity measurements in the observatory of the GvN station on the Ekström ice shelf in the Antarctic are strongly influenced by the local sea level, as expected. Vertical movements at the GvN station are derived from the observed gravity records. These are 33 cm for M_2 and 23 cm for O_1 as an example.

The vertical movements of the ice shelf were modelled under the assumption of uniform slab hinged at one side and vertically displaced by the sea tide and a best fit between the observed and modelled amplitudes of the main-earth tidal waves could be achieved. The hypothetical hinge zone was also determined. A simple elastic model places it 55 km south of the GvN station. According to this model no vertical movements due to the local ocean tides are to be expected south of this zone.

The present model for the Ekström ice shelf is a first preliminary attempt to explain the vertical movements observed at GvN. Of course, the Ekström ice shelf is not a

rectangular body of ice as assumed. But neverthelss the model is a good compromise regarding the information available: one yearly record of sea level, and gravity measurements at only one point of an ice plate with rather complicated boundaries. The refinement of the model and its extension into two or even three dimensions could be accomplished without much difficulty. The verification of a more complex model would require more observation sites for gravity records on the ice. Logistically and financially this would be very difficult to achieve.

ACKNOWLEDGMENTS

The authors are greatly indebted to Dr W. Zürn, Prof. Dr G. Krause, Prof. Dr R. Ramseier and Prof. Dr G. Jentzsch for many stimulating discussions and for reading the manuscript. They are grateful to Prof. Dr H. Miller and Dr A. Brodscholl for the gravity tidal data that was analysed in this paper. The Askania GS-15 gravimeter in the observatory of GvN was borrowed from the observatory Schiltach. Computations were carried out on the CONVEX C210S in the GSF-Forschungszentrum für Umwelt und Gesundheit, Braunschweig, and on the VAX 6520 VP in the Alfred-Wegener-Institut, Bremerhaven. At least two anonymous reviewers are kindly acknowledged for helping very much to improve the paper. This paper is AWI contribution 528.

REFERENCES

Bishop, J. F. & Walton, J. L. W., 1977. Problems encountered when monitoring tidal movements in extremely cold regions, *Polar Record,* **18,** 116, 502–505.

Cartwright, D. E. & Edden, A. C., 1973. Corrected tables of tidal harmonics, *Geophys. J. R. astr. Soc.,* **33,** 253–264.

Cartwright, D. E. & Tayler, R. J., 1971. New computations of the tide generating potential, *Geophys. J. R. astr. Soc.,* **23,** 45–74.

Dubrovin, L. I. & Simonov, I. M., 1965. Tides in the Novolazarevskaja station area, *Soviet Antarc. Exped. Inf. Bull.,* **5,** 272–275.

Eckstaller, A. & Miller, H., 1984. Gezeitenvertikalbewegung des Filchner Schelfeises, *Ber. z. Polarforschung,* **19,** 82–97.

Holdsworth, G., 1969. Flexure of a floating ice tongue, *J. Glaciol.,* **8,** 54, 385–397.

Holdsworth, G., 1977. Tidal interaction with ice shelves, *Ann. Geophys.,* **33,** 133–146.

Hughes, T., 1975. The West Antarctic ice sheet: instability, disintegration and iniation of ice ages, *Rev. Geophys. Space Phys.,* **13,** 502–526.

Hughes, T., 1977. West Antarctic ice streams, *Rev. Geophys. Space Phys.,* **15,** 1–46.

Kobarg, W., 1988. Die gezeitenbedingte Dynamik des Ekström-Schelfeises, Antarktis, *Ber. z. Polarforschung,* **50.**

Kobarg, W. & Lippmann, E., 1986. Gezeitenmessungen auf dem Ekström-Schelfeis, Antarktis, *Polarforschung,* **56,** 1–21.

Krause, G., 1988. Water level measurements in the Weddel sea, *IOC Workshop Report,* **54,** 22–25.

Lingle, C. S., Hughes, T. J. & Kollmeier, R. J., 1981. Tidal flexure of Jacobshavns glacier, West Greenland, *J. geophys. Res.,* **86,** 3960–3968.

Melchior, P., 1982. *Tides of the Planet Earth,* Pergamon Press, Oxford.

Mende, D. & Simon, G., 1969. *Physik-Gleichungen und Tabellen,* VEB Fachbuchverlag, Leipzig.

Pratt, J. G. D., 1960. Tides at the Shackleton, Weddel Sea, Transantarctic Expedition 1955–1958, *Sci. Rep.,* **4.**

Robin, G. de Q., 1958. Seismic shooting and related investigations, Norw.-Brit.-Swed. Ant. Exp., 1949–1952, *Scientfic Results.,* **V,** Glaciology 3, Oslo.

Robinson, E. S., Williams, R. T., Neuburg, H. A. C., Rohrer, C. S. & Ayers, R. L., 1977. Interaction of the ocean tide and solid earth tide in the Ross Sea Area of Antarctica. Preliminary results, *Ann. Geophys.,* **33,** 147–150.

Rydelek, P. A., Knopoff, L. & Zürn, W., 1982. Observations of 18.6-year modulation tide, *J. geophys. Res.,* **87,** 5535–5537.

Schüller, K., 1976. Ein Beitrag zur Auswertung von Erdgezeitenregistrierungen, *Deutsche Geodätische Komm. d. Bay. Akad. d. Wiss.,* Reihe C, **227.**

Schüller, K., 1978. Principles of the HYCON method, *Bulletin d'Informations Merées Terrestres,* **78,** 4667–4669.

Thiel, E., Crary, A. P., Haubrich, R. A. & Behrendt, J. C., 1960. Gravimetric determination of ocean tide, Weddel and Ross seas, Antarctica, *J. geophys. Res.,* **65,** 629–636.

Thyssen, F. & Grosfeld, K., 1988. Ekström ice shelf, *Ann. Glaciol.,* **11,** 180–183.

Wahr, J. M., 1981. Body tides on an elliptical, rotating, elastic and oceanless Earth, *Geophys. J. R. astr. Soc.,* **64,** 677–703.

Wilhelm, H. & Zürn, W., 1984. Tides of the earth, in: *Landolt-Börnstein, Zahlenwerke und Funktionen aus Naturwissenschaften und Technik,* **V 2a,** Heidelberg, pp. 259–299.

Williams, R. T. & Robinson, E. S., 1979. Ocean tide and waves beneath the Ross ice shelf, Antarctica, *Science,* **203,** 443–445.

Yarmanci, U., 1978. Spectral interpretation of the error calculation in tidal analysis, *Bulletin d'Informations Marées Terrestres,* **78,** 4676–4683.

Zürn, W., Beaumount, C. & Slichter, L. B., 1976. Gravity tides and ocean loading in southern Alaska, *J. geophys. Res.,* **81,** 4923–4932.